

Nature of energy transfer processes in F -center– CN^- -defect pairs in CsCl

G. Halama

Physics Department, Arizona State University, Tempe, Arizona 85287-1504

S. H. Lin

Chemistry Department, Arizona State University, Tempe, Arizona 85287-1604

K. T. Tsen

Physics Department, Arizona State University, Tempe, Arizona 85287-1504

F. Luty

Physics Department, University of Utah, Salt Lake City, Utah 84112

J. B. Page

Physics Department, Arizona State University, Tempe, Arizona 85287-1504

(Received 18 September 1989)

A model which considers the F center and a nearby CN^- molecule as a whole entity (or “super-molecule”) has been proposed to explain the observed anti-Stokes resonance Raman scattering of F -center– CN^- -defect pairs in CsCl. It is demonstrated that the vibrational-vibrational energy transfer process has to be properly taken into account in order to obtain a satisfactory fit of the relative magnitudes of the various transitions as measured in the Raman experiments.

I. INTRODUCTION

When an electron is trapped at a negative-ion vacancy in an alkali halide crystal, a point imperfection with a simple electronic structure and high symmetry is established. Such crystalline defects are usually referred to as F centers. It has recently been demonstrated¹ that the F center can be associated with various cationic or anionic point defects. Unlike isolated F centers, whose properties are now well understood,² these new F -aggregate centers of reduced local symmetry provide relatively simple and interesting physical systems for both theoreticians and experimentalists to investigate a variety of fundamental energy-transfer processes in solids. For instance, electronic (e) excitation of such F -aggregate centers by optical irradiation with laser light produces electronic-to-vibrational (e - v) energy transfer into the stretching mode (v) of the attached molecular defect.^{3,4} These excited vibrational modes can decay by transferring their energy to nearby isolated molecules through the vibrational to vibrational (v - v) energy-transfer process.⁵ Although much progress has been made in understanding the overall behavior of this important class of defect, very little is known about the microscopic nature of their e - v and v - v energy-transfer processes. Among these F -aggregate centers, F -center– CN^- -defect pairs [$F_{\text{H}}(\text{CN}^-)$] and F -center– OH^- -defect pairs [$F_{\text{H}}(\text{OH}^-)$] have been the most extensively studied.^{1,6} Recently, we have analyzed both the e - v and v - v energy-transfer processes in $F_{\text{H}}(\text{OH}^-)$ defects in KCl in terms of the Dexter-Förster mechanism^{7,8} and have demonstrated this mechanism to be appropriate for both energy-transfer processes. However, this

dipole-dipole interaction mechanism has been found⁹ to be unable to explain the infrared vibrational emission spectra of the $F_{\text{H}}(\text{CN}^-)$ system observed by Yang and Luty,³ and so we have not applied this mechanism to our observed anti-Stokes Raman data. In this paper, we propose a new model, which considers the F center and associated CN^- defect as a whole entity or “supermolecule,” to account for the measured⁴ anti-Stokes Raman scattering of $F_{\text{H}}(\text{CN}^-)$ defects in CsCl.

II. THEORY

The total differential scattering cross section per unit solid angle per unit frequency for resonance Raman scattering is given by¹⁰

$$\frac{\delta^2 \sigma}{\delta \Omega \delta \omega_2} = \sum_{(a,u)} \rho_{a,u} \frac{\delta^2 \sigma_{a,u;a,v}}{\delta \Omega \delta \omega_2}, \quad (1)$$

where $\delta^2 \sigma_{a,u;a,v} / \delta \Omega \delta \omega_2$ is the differential scattering cross section for a transition from the (a,u) state to the (a,v) state, $\rho_{a,u}$ is the initial population of the (a,u) state, $|a\rangle$ is the electronic part of the wave function, $|u\rangle$ and $|v\rangle$ are vibrational wave functions for the crystal in the adiabatic approximation, ω_2 is the scattered-light frequency, and Ω is the solid angle. We will show in the following sections the derivation of expressions for (1) the initial populations $\rho_{a,u}$ using the density-matrix formalism, (2) the electronic-to-vibrational transition rates involved in the density-matrix formalism, and (3) the single-level resonant Raman-scattering (RRS) cross section.

A. Time evolution of the density matrix

First, let us determine the population of the various states by using the stochastic Liouville equation¹¹

$$\frac{\delta\rho}{\delta t} = -iL\rho - i[V, \rho]/\hbar - \Gamma\rho, \quad (2)$$

where ρ is the density-matrix operator, L is the Liouville operator of the system, $V = D(\omega_r)\exp(-i\omega_r t) + D(-\omega_r)\exp(i\omega_r t)$ is the interaction energy of the incident radiation field, and Γ describes the damping of the system.

We would like to apply the Liouville equation to the energy decay in Fig. 1. In our model the incident radiation pumps our system from the electronic ground state (g) to one of two electronic excited levels $F_H(1)$ or $F_H(2)$. Then the electron decays quickly to the relaxed electronic excited configuration (a). From (a) the electronic energy can be transferred to the vibrational stretching mode of the CN⁻ molecules. To a good approximation, for insulators such as alkali halides the wave functions are given by the adiabatic approximation. The time evolution of the diagonal density-matrix element of the a th electronic state is given by

$$\frac{\delta\rho_{aa}}{\delta t} + (i/\hbar)(V_{ag}\rho_{ga} - \rho_{ag}V_{ga}) + \Gamma_{aa}^{\rho_{aa}} = 0, \quad (3)$$

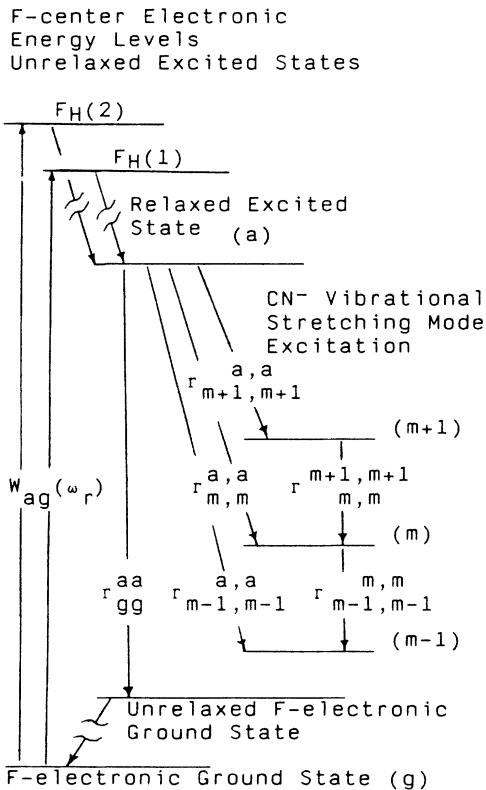


FIG. 1. Model for the electronic-vibrational energy transfer in $F_H(\text{CN}^-)$ defect pairs in CsCl (see text for discussion).

where ρ_{aa} is the diagonal matrix element for the a th electronic state, ρ_{ag} and ρ_{ga} are off-diagonal elements between the a th and g th electronic states, V_{ag} and V_{ga} are the coupling matrix elements due to the radiation field, $\Gamma_{aa}^{\rho_{aa}}$ is the sum over all the possible decays out of the excited state a . Now consider the off-diagonal elements between the a th and g th electronic states,

$$\frac{\delta\rho_{ag}}{\delta t} + i\omega_{ag}\rho_{ag} + (i/\hbar)V_{ag}(\rho_{gg} - \rho_{aa}) + \Gamma_{ag}^{\rho_{ag}} = 0, \quad (4)$$

where $\omega_{ag} = (E_a - E_g)/\hbar$, E_a and E_g are the eigenenergies of the respective states, and $\Gamma_{ag}^{\rho_{ag}}$ denotes the dephasing constant for these transitions. If we substitute the explicit expression for V , calculate the elements V_{ag} and V_{ga} , and use the rotating-wave and steady-state approximations, we get¹¹

$$\rho_{ag}(\omega_r) = \frac{-i(\rho_{gg} - \rho_{aa})}{\hbar} \frac{D_{ag}(\omega_r)}{i(\omega_{ag} - \omega_r) + \Gamma_{ag}^{\rho_{ag}}}, \quad (5)$$

where $D_{ag}(\omega_r) = \langle a | D(\omega_r) | g \rangle$. To obtain these matrix elements, we have made the Condon approximation so that the electronic states $|a\rangle$ and $|g\rangle$ are appropriate to the atomic equilibrium configuration $R=0$ in the electronic ground state. Then we substitute Eq. (5) into Eq. (3) to get

$$\frac{\delta\rho_{aa}}{\delta t} + W_{ag}(\omega_r)(\rho_{aa} - \rho_{gg}) + \Gamma_{aa}^{\rho_{aa}} = 0, \quad (6)$$

where $W_{ag}(\omega_r)$ represents the rate constant for absorption.

Next, we consider the matrix elements for the vibrational states

$$\frac{\delta\rho_{mm}}{\delta t} + \Gamma_{mm}^{\rho_{aa}}\rho_{aa} + \Gamma_{m,m}^{m,m}\rho_{m,m} + \Gamma_{m,m}^{m+1,m+1}\rho_{m+1,m+1} = 0, \quad (7)$$

where the indices m and a stand for the excitation level of the vibrational stretching mode for the CN⁻ and the relaxed electronic excited state, respectively, $\Gamma_{mm}^{\rho_{aa}}$ denotes the radiationless transition rate from the electronic state to the m th vibrational excitation, $\Gamma_{m,m}^{m+1,m+1}$ denotes the transition rate from the $(m+1)$ th vibrational state to the m th vibrational state, and $\Gamma_{m,m}^{m,m}$ is the transition rate for all possible decays out of the m th vibrational state.

Equations (6) and (7) will be the master equations used to analyze the experimental results for either time-resolved spectroscopy or steady-state spectroscopy. For our experimental conditions of Ref. 4, it is appropriate to use the steady-state solutions of Eqs. (6) and (7). They are

$$\rho_{aa} = \frac{W_{ag}(\omega_r)\rho_{gg}}{W_{ag}(\omega_r) + \Gamma_{aa}^{\rho_{aa}}} \quad (8)$$

and

$$\rho_{m,m} = -\frac{\Gamma_{mm}^{\rho_{aa}}\rho_{aa} + \Gamma_{m,m}^{m+1,m+1}\rho_{m+1,m+1}}{\Gamma_{m,m}^{m,m}}, \quad (9)$$

where the absorption rate $W_{ag}(\omega_r)$ is given by

$$W_{ag}(\omega_r) = \frac{2}{\hbar^2} \frac{|\langle a|D(\omega_r)|g\rangle|^2 \Gamma_{ag}}{\Gamma_{ag}^2 + (\omega_{ag} - \omega_r)^2}. \quad (10)$$

B. Electronic-to-vibrational (e - v) transfer rate

Next, we discuss the calculation of the electronic relaxation (a, ν) \rightarrow (g, μ). The radiationless transition-rate constant can be expressed using the Fermi golden rule and has the form¹²⁻¹⁴

$$W_{a,0;g,m} = \frac{2\pi}{\hbar} \sum_{\nu} \sum_{\mu} P_{a,\nu} |\langle g, \mu | \hat{H}' | a, \nu \rangle|^2 \delta(E_{a,\nu} - E_{g,\mu}), \quad (11)$$

where \hat{H}' denotes the perturbation for electronic relaxation and $P_{a,\nu}$ represents the Boltzmann distribution. In evaluating $W_{a,0;g,m}$, the adiabatic approximation is generally used for the basis set.¹⁵ In this case the wave functions $|a, \nu\rangle$ and $|g, \mu\rangle$ can be written as products of electronic wave functions $\psi_a(r, R)$ and $\psi_g(r, R)$ and vibrational wave functions $\theta_{a,\nu}(R)$ and $\theta_{g,\mu}(R)$, i.e.,

$$|a, \nu\rangle = \psi_a \theta_{a,\nu}, \quad |g, \mu\rangle = \psi_g \theta_{g,\mu}. \quad (12)$$

The respective eigenenergies ($E_{a,\nu}$ and $E_{g,\mu}$) of these wave functions are given by

$$E_{g,\mu} = E_g + (m + \frac{1}{2})\hbar\omega' + \sum_j (\mu_j + \frac{1}{2})\hbar\omega_j \quad (13)$$

and

$$E_{a,\nu} = E_a + \frac{1}{2}\hbar\omega' + \sum_j (\nu_j + \frac{1}{2})\hbar\omega_j, \quad (14)$$

where E_a and E_g are the electronic energies, ω' is the CN^- stretching-mode frequency, and the ω_j 's are all of the other vibrational frequencies of the lattice. We are assuming that the normal coordinates in the ground and excited electronic states are the same except for shifted equilibrium positions (displaced-oscillator model). Thus the ω_j 's are the same in Eqs. (13) and (14). \hat{H}' is the kinetic-energy operator for the nuclear motion and we have, approximately,

$$\begin{aligned} & \langle \psi_g \theta_{g,\mu} | \hat{H}' | \psi_a \theta_{a,\nu} \rangle \\ &= - \sum_j \hbar^2 \langle \theta_{g,\mu} | \delta \theta_{a,\nu} / \delta q_j \rangle \langle \psi_g | \delta \psi_a / \delta q_j \rangle, \end{aligned} \quad (15)$$

where the q_j 's denote the vibrational normal coordinates.

We now apply Eqs. (11)–(13) to our problem. We first consider the $T=0$ K case. We shall let $\chi_{a,0}$ and $\chi_{g,m}$ denote the vibrational wave functions of the CN^- . In this case, Eq. (11) can be written as

$$W_{a,0;g,m} = \frac{2\pi}{\hbar} |R_i(g, a)|^2 |\langle \chi_{g,m} | \chi_{a,0} \rangle|^2 \sum_{\mu} |\langle \chi_{g,\mu} | \delta \chi_{a,0} / \delta q_i \rangle|^2 \prod_{\substack{j \\ (j \neq i)}} |\langle \chi_{g,\mu_j} | \chi_{a,0_j} \rangle|^2 \delta(E_{a,0} - E_{g,\mu}), \quad (16)$$

where

$$|\langle \chi_{g,m} | \chi_{a,0} \rangle|^2 \quad \text{and} \quad |\langle \chi_{g,\mu_j} | \chi_{a,0_j} \rangle|^2 \quad (17)$$

are the Franck-Condon factors, and

$$R_i(g, a) = -\hbar^2 \langle \psi_g | \delta \psi_a / \delta q_i \rangle. \quad (18)$$

Here, for simplicity it is assumed that there is one promoting mode. Using the displaced-oscillator model, we obtain

$$W_{a,0;g,m} = \frac{2\pi}{\hbar} \left[\frac{\alpha_i}{2} \right] |R_i(g, a)|^2 \frac{(S')^m e^{-S'}}{m!} \sum_{\mu} \left[\prod_{\substack{j \\ (j \neq i)}} \frac{(S_j)^{\mu_j} \exp(-S_j)}{\mu_j!} \right] \delta(E_{a,0} - E_{g,\mu}), \quad (19)$$

where $\alpha_i = \omega_i / \hbar$ and the S_j 's are the dimensionless normal coordinate displacements under electronic excitation (i.e., electron-phonon-coupling constants). By using the integral representation for the δ function, we find for the strong-coupling case

$$W_{a,0;g,m} = \frac{|R_i(g, a)|^2 \alpha_i}{2\hbar^2} \frac{(S')^m}{m!} e^{-S'} \left[\frac{2\pi}{\sum_j S_j \omega_j^2} \right]^{1/2} \exp \left[- \frac{[\omega_{a,g} - \omega_i - m\omega' - \sum_j S_j \omega_j]^2}{2 \sum_j S_j \omega_j^2} \right], \quad (20)$$

where S' and ω' are the coupling constant and frequency for the CN^- stretching mode, ω_i is the frequency of the promoting mode, and S_j and ω_j are the coupling constants and frequencies for the phonon modes. If the temperature dependence of the electronic relaxation is included, $W_{a,0;g,m}$ is given by¹⁶

$$W_{a,0;g,m} = \frac{|R_i(g, a)|^2 \alpha_i}{2\hbar^2} \frac{(S')^m}{m!} e^{-S'} \left[\frac{2\pi}{\sum_j (2n_j + 1) S_j \omega_j^2} \right]^{1/2} \exp \left[- \frac{[\omega_{a,g} - \omega_i - m\omega' - \sum_j S_j \omega_j]^2}{2 \sum_j (2n_j + 1) S_j \omega_j^2} \right], \quad (21)$$

where n_j denotes the thermal-equilibrium number of phonons in the j th mode,

$$n_j = \left[\exp \left(\frac{\hbar \omega_j}{kT} \right) - 1 \right]^{-1}. \quad (22)$$

C. Calculation of the resonance Raman scattering

Now the calculation of the differential scattering cross section for a transition from the (au) state to the (av) state will be shown. Using the Green's-function method,¹⁷ the rotating-wave approximation, the adiabatic approximation for the wave functions,¹⁵ and the Condon approximation, we find that the resonance Raman differential scattering cross section is given by

$$\frac{\delta \sigma_{a,u;a,v}^2}{\delta \Omega \delta \omega_2} = \frac{\omega_1 \omega_2^3 |\mu_1|^2 |\mu_2|^2 \Gamma_{a,u;a,v} |Z_{a,u;a,v}|^2}{\pi \hbar^2 c^4 [(\omega_{a,u;a,v} - \omega_1 + \omega_2)^2 + \Gamma_{a,u;a,v}]} \quad (23)$$

where μ_1 and μ_2 are the electronic-transition dipole-moment matrix elements, $\omega_{a,u;a,v}$ is the frequency of the Raman shift, ω_1 and ω_2 are the incident and scattered light frequencies, respectively, and

$$Z_{a,u;a,v} = \sum_{n=0}^{\infty} \frac{\langle u|n\rangle \langle n|v\rangle}{i(\omega_{b,n;a,u} - \omega_1) + \Gamma_{b,n;a,u}}. \quad (24)$$

Here, $\langle u|n\rangle$ and $\langle n|v\rangle$ are vibronic overlap integrals. Following Refs. 17–19, a detailed multimode derivation of $Z_{a,u;a,v}$ can be obtained, and we sketch a derivation in the Appendix.

D. Theoretical analysis

To perform the theoretical analysis, we need to combine the results of Secs. II A–II C. Then we can calculate the relative magnitudes of the various vibronic peaks in the Raman spectra.

To calculate the population of the various vibrational excitations, we will use Eq. (9) from Sec. II A. To simplify the analysis, we will let the total decay rate $\Gamma_{m+1,m+1}^{m+1,m+1}$ be equal to the single-level decay rate $\Gamma_{m,m}^{m+1,m+1}$. Thus Eq. (9) from Sec. II A becomes

$$\rho_{m,m} = - \frac{\Gamma_{mm}^{aa} \rho_{aa} - \Gamma_{m+1,m+1}^{m+1,m+1} \rho_{m+1,m+1}}{\Gamma_{m,m}^{m,m}}. \quad (25)$$

We already have derived an expression for the (e - v) transition rate in Sec. II B, but will now simplify Eq. (21) of that section by letting $\sum_j S_j \omega_j^2 (2n_j + 1) \rightarrow S \omega^2 [2n(\omega) + 1]$, where ω is the average phonon frequency, S is an effective electron-phonon-coupling constant for the F center, and $n(\omega)$ is the thermal population at the average phonon frequency. Then, Eq. (21) becomes

$$W_{a,0;g,m} = A \left[\frac{2\pi}{S \omega^2 [2n(\omega) + 1]} \right]^{1/2} \frac{(S')^m}{m!} \times \exp \left[- \frac{(\omega_{a,g} - S \omega - \omega_i - m \omega')^2}{2S \omega^2 [2n(\omega) + 1]} \right], \quad (26)$$

where

$$A = \frac{|R_i(g,a)|^2 \omega_i}{2\hbar^3} \quad (27)$$

will be taken to be constant and we assume that the promoting-mode frequency ω_i is the average phonon frequency ω . Here the decay rates of the vibrational levels of the CN⁻, $\Gamma_{m,m}^{m,m}$, are composed of two decay rates. One of them, denoted W_m , will be a proportionality constant B times the quantum number m of the vibrational excitation. The other rate, denoted $W_{v,m}$, accounts for the v - v energy transfer²⁰ from the F_H (CN⁻) centers into the isolated CN⁻ molecules, due to the high concentration (10^{19} CN⁻/cm³) of CN⁻ molecules in the sample used in the experimental measurements. In other words, we have

$$W_m = mB, \quad (28)$$

and, to a single phonon-assisted approximation,²⁰

$$W_{v,m} = C \frac{mD(\Delta\omega_m)n(\Delta\omega_m)}{\omega_A \omega_{D,m}}, \quad (29)$$

where m is the quantum number of the vibrational level, ω_A is the acceptor stretching-mode frequency (the frequency for the transition from the 0 to 1 levels of the free CN⁻ molecule), $\omega_{D,m}$ is the donor stretching-mode frequency (the frequency for a transition from the m th to the $(m-1)$ th level for the CN⁻ molecule aggregated to the F center), $\Delta\omega_m = \omega_A - \omega_{D,m}$, $D(\Delta\omega_m)$ is the phonon density of states at $\Delta\omega_m$, $n(\Delta\omega_m)$ is the thermal phonon population at $\Delta\omega_m$, and B and C are constants that determine the strengths of the respective transition rates. It then follows that

$$\Gamma_{m,m}^{m,m} = W_m + W_{v,m}. \quad (30)$$

If we substitute $\Gamma_{mm}^{aa} = -W_{a,0;g,m}$ and Eq. (30) into Eq. (25), then the relative populations of the CN⁻ molecule aggregated to the F center can be calculated by using

$$\rho_{mm} = \frac{W_{a,0;g,m} \rho_{aa} + (W_{m+1} + W_{v,m+1}) \rho_{m+1,m+1}}{W_m + W_{v,m}}. \quad (31)$$

Now we can combine the single-level RRS differential cross section and Eq. (31) to get the relative magnitudes of the various RRS transitions.

III. COMPARISON OF THEORETICAL CALCULATIONS AND EXPERIMENTAL RESULTS

For all of the RRS theoretical calculations, the anharmonic shifts of the various transitions⁴ are set at 25 cm^{-1} , the incident laser frequency ω_1 is $18\,797 \text{ cm}^{-1}$, the maximum absorption frequency⁵ ω_{MA} is $17\,144 \text{ cm}^{-1}$, the full width at half maximum⁵ (FWHM) is 1700 cm^{-1} , and $\Gamma_{a,u;a,v}$ is chosen to fit the half-width of the anti-Stokes RRS signal, which was resolution-limited by the instruments. Figure 2 shows the measured anti-Stokes Raman signal for F_H (CN⁻) defect pairs²¹ in CsCl at $T \approx 20 \text{ K}$. The parameter set which gives the best fit to these experimental results is $\omega_{a,g} = 13\,500 \text{ cm}^{-1}$, $\omega = 121 \text{ cm}^{-1}$,

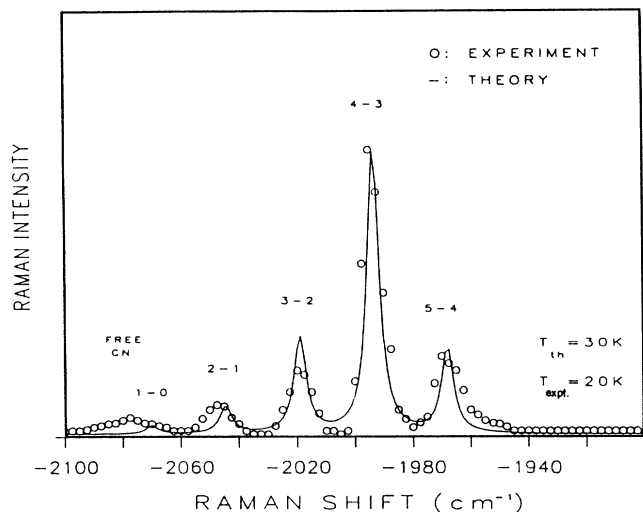


FIG. 2. Anti-Stokes resonance Raman-scattering spectrum (open circles) of $F_H(\text{CN}^-)$ defect pairs in CsCl taken at $T \approx 20$ K and with $\lambda_{\text{laser}} = 532$ nm. The solid curve represents the best theoretical fit from the model calculations.

$S = 30$, $S_m = 0.2$, $C/B = 2.93 \times 10^{-17} \text{ s}^{-3}$, and $T = 30$ K, together with the weighted relative phonon density of states for the various phonon frequencies involved in the calculations of v - v energy transfer, as given in Table I. We notice that the first three parameters are very close to the corresponding values found for pure F centers.²

To demonstrate the importance of including the v - v energy-transfer process in the theoretical calculations, we have plotted in Fig. 3 a typical theoretical curve which does *not* take into account the v - v energy-transfer process. The parameter values are those of the preceding paragraph, except that $T = 20$ K and $C = 0$. It has been found that no matter how the parameters are adjusted, the magnitudes of the lower excitation transitions ($m \leq 3$) are always either comparable to or larger than that of the 4-3 transition. Consequently, it is essential to consider the v - v energy-transfer process to understand our experimental results.

Figure 4(a) shows a reasonable fit obtained with the parameter set $\omega_{a,g} = 13\,500 \text{ cm}^{-1}$, $\omega = 121 \text{ cm}^{-1}$, $S = 33$,

TABLE I. Weighted relative phonon density of states used in the calculations of the phonon-assisted v - v energy-transfer process.

| Excitation level of CN^- (m) | Phonon frequency ($\Delta\omega_m$) (cm^{-1}) | Weighted relative density of states $D(\Delta\omega_m)$ |
|---|--|---|
| 1 | 10 | 1 |
| 2 | 35 | 2 |
| 3 | 60 | 2 |
| 4 | 85 | 1 |
| 5 | 110 | 1 |

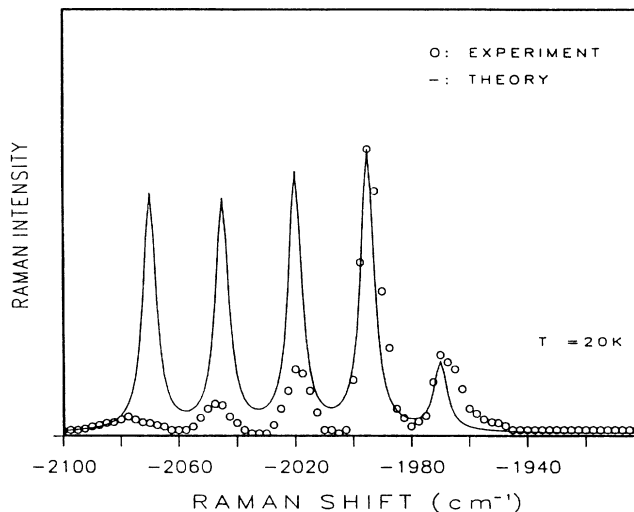


FIG. 3. Theoretical calculation of anti-Stokes resonance Raman scattering spectrum (solid curve), which does not include the v - v energy-transfer process. The open circles are the experimental data of Fig. 2, shown here for comparison. The temperature is 20 K for both the theory and the experiment.

and $S_m = 0.2$; the v - v transition-rate parameters are $C/B = 4.78 \times 10^{-17} \text{ s}^{-3}$ and $T = 15$ K. The phonon density of states used for these calculations is given by the Debye model,²² i.e., $D(\Delta\omega_m) \propto (\Delta\omega_m)^2$. However, we expect that if our theoretical calculations are appropriate, they should also be able to describe the temperature dependence (primarily arising from the phonon-assisted

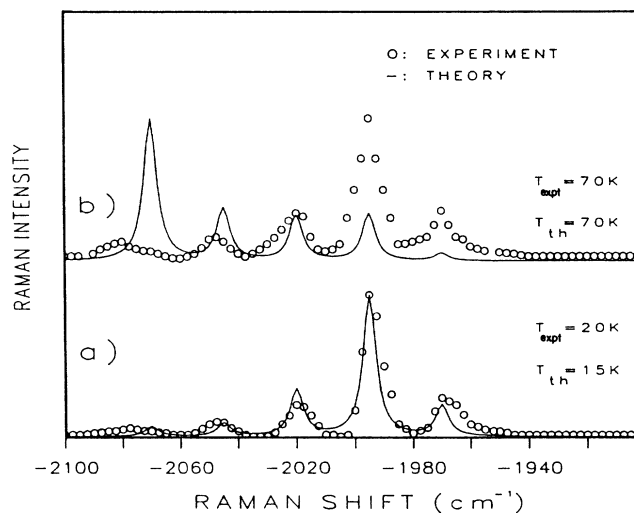


FIG. 4. Anti-Stokes resonance Raman-scattering spectra (open circles) for $F_H(\text{CN}^-)$ defect pairs in CsCl taken at (a) $T \approx 20$ K and (b) $T \approx 70$ K, respectively. The solid curve corresponds to the theoretical calculations based on the phonon-frequency density of states from the Debye model (see text for discussion).

v - v energy-transfer process) of the anti-Stokes RRS signal. As shown in Fig. 4(b), at $T=70$ K the theoretical calculations using the above parameter set, including the phonon density of states given by Debye model, predict a much more dramatic change of the relative intensities of the Raman peaks for various transitions when compared with the $T=70$ K experimental data. Of course, a realistic curve of the phonon-frequency density of states in a crystal is not as smooth and monotonic as predicted by the Debye model, but typically contains many sharp structures. Consequently, it is not surprising that we find that a weighted relative phonon density of states such as the one given in Table I gives a better fit than those of the Debye model.

Figures 5(a)–5(c) show that, by using weighted relative phonon densities of states in the theoretical calculations, we can both fit the experimental anti-Stokes RRS signal at $T \approx 20$ K and account for the temperature dependence. Figure 5(a) is identical to Fig. 2, and the only parameter varied in the theoretical calculations for Figs. 5(b) and 5(c) was the temperature. We do not try to fit the data taken at temperatures higher than $T \approx 120$ K with our theory because the aggregation of the F centers to the CN^- molecules occurs at $T \sim 150$ K. We estimate that our measured temperatures have an uncertainty of about ± 10 K. On the other hand, our temperature variation for a good theoretical fit to the experimental results is about ± 5 K. The sizable discrepancy in temperature between the experimental results and the theoretical calculations for $T \geq 100$ K is most likely caused by the effect of disassociation of CN^- molecules from F centers at such temperatures.

It is interesting to compare the weighted relative phonon densities of states (1:2:2:1:1) that were found to best fit our experimental data with those (1:4:11:1:10) calculated by Ahmad *et al.*²³ with an 11-parameter shell model for pure CsCl. We believe that the difference is most likely to be due to the defects (i.e., CN^- molecules and F centers) in the CsCl crystals of our experiments.²⁴

It should be noted that with our best-fit parameter set, our model predicts the appearance of extremely weak shoulders on the high-energy side of the absorption spectra for both the $F_H(1)$ and $F_H(2)$ absorption bands. However, because of (1) the overlap of the $F_H(1)$ and $F_H(2)$ absorption bands, and (2) the width of each individual absorption band, the weak shoulders for the $F_H(1)$

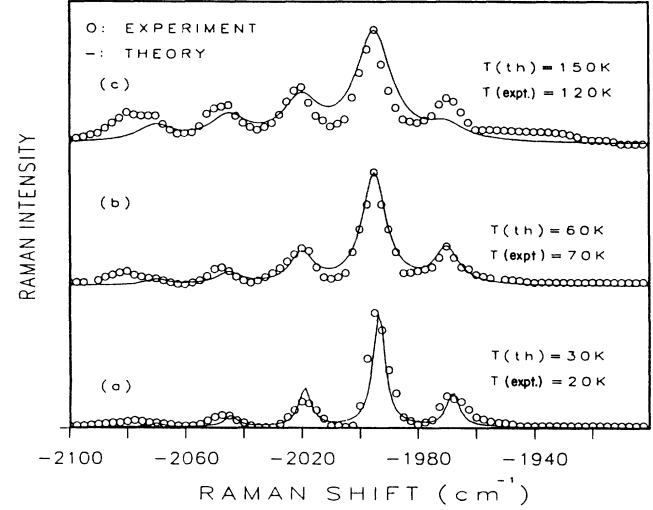


FIG. 5. Anti-Stokes resonance Raman spectra (open circles) of $F_H(\text{CN}^-)$ defects pairs in CsCl taken at (a) $T \approx 20$ K, (b) $T \approx 70$ K, and (c) $T \approx 120$ K, respectively. The solid curves represent the theoretical calculations based on the weighted relative phonon density of states as given in Table I and discussed in the text.

and $F_H(2)$ absorption bands would be very difficult to detect experimentally.

IV. CONCLUSIONS

In conclusion, we have developed a new model which considers the F center and its aggregated CN^- molecule as a whole entity (or supermolecule) to explain the measured temperature-dependent anti-Stokes RRS spectra of $F_H(\text{CN}^-)$ defect pairs in CsCl. We have shown that it is essential to take into account the v - v energy-transfer process between the F -aggregate CN^- molecules and the nearby isolated CN^- molecules. Time-resolved RRS experiments are underway to further test our model.

ACKNOWLEDGMENTS

This work was supported by the U.S. National Science Foundation under Grants No. DMR-87-18228, No. DMR-87-06416, and No. CHE-86-10104.

APPENDIX: CALCULATION OF $Z_{a,u;a,v}$

This derivation follows that of Ref. 17. If we use

$$\frac{1}{a+ib} = -i \int_0^{\infty} \exp[i(a+ib)t] dt \quad (\text{A1})$$

in Eq. (24) of Sec. II C, then

$$Z_{a,u;a,v} = -i \int_0^{\infty} dt \exp[-i(\omega_{ba} - \omega_1)t + i(v_m + \frac{1}{2})\omega_m t - \gamma t] (B_j)(B_m), \quad (\text{A2})$$

where $\Gamma_{b,m;a,u}$ is equal to γ for all transitions,

$$B_j = \prod_j \sum_{v_j'} e^{-i\omega_j v_j' t} \langle a, 0 | b, v_j' \rangle \langle b, v_j' | a, 0 \rangle, \quad (\text{A3})$$

and

$$B_m = \sum_{v'_m} e^{-i\omega_m(v'_m + 1/2)t} \langle a, u_m | b, v'_m \rangle \langle b, v'_m | a, v_m \rangle. \quad (\text{A4})$$

In Eqs. (A2)–(A4), ω_{ab} is the electronic transition energy between the minima of the excited states and the ground state (i.e., zero-phonon energy), the subscript m labels the states of the CN^- stretching mode, and the subscript j labels all the phonon modes coupled to the F -center electron. First, we will work on B_m in Eq. (A4), suppressing the subscript m and substituting the harmonic-oscillator wave functions,

$$\begin{aligned} |a, v\rangle &= \frac{(\alpha/\pi)^{1/4}}{(2^v v!)^{1/2}} e^{-\alpha r^2/2} H_v(\sqrt{\alpha}r), & \langle a, u| &= \frac{(\alpha/\pi)^{1/4}}{(2^u u!)^{1/2}} e^{-\alpha s^2/2} H_u(\sqrt{\alpha}s), \\ |b, v'\rangle &= \frac{(\alpha/\pi)^{1/4}}{(2^{v'} v'!)^{1/2}} e^{-\alpha (s')^2/2} H_{v'}(\sqrt{\alpha}s'), & \langle b, v'| &= \frac{(\alpha/\pi)^{1/4}}{(2^{v'} v'!)^{1/2}} e^{-\alpha (r')^2/2} H_{v'}(\sqrt{\alpha}r'). \end{aligned} \quad (\text{A5})$$

We also use Mahler's formula,

$$\sum_v \frac{e^{-\mu(v+1/2)}}{\sqrt{\pi} 2^v v! e^{(x^2+y^2)/2}} H_v(x) H_v(y) = \frac{\exp\left[-\frac{(x+y)^2 \tanh(\mu)}{4} - \frac{(x-y)^2 \coth(\mu)}{4}\right]}{[2\pi \sinh(\mu)]^{1/2}}, \quad (\text{A6})$$

to do the summation over v' , giving

$$B_m = D \int_{-\infty}^0 dx \int_{-\infty}^0 dy H_u(x) H_v(y) e^{-(x^2+y^2)/2} \exp\left[-\frac{(x'+y')^2 \tanh(\mu) + (x'-y')^2 \coth(\mu)}{4}\right], \quad (\text{A7})$$

where $D = [2\pi^2 \sinh(\mu) 2^{(u+v)v!u!}]^{-1/2}$, $\mu = i\omega_m t$, $H_u(x)$ and $H_v(y)$ are Hermite polynomials, $x = \sqrt{\alpha}r$, $x' = r + q$, $y = \sqrt{\alpha}s$, $y' = s + q$, $\alpha = \hbar\omega_m/M$ in the displaced-oscillator model $q = \sqrt{\alpha}d$, M is the reduced mass of the oscillator, ω_m is the angular frequency of oscillation, and d is the increase in the bond length of the high-frequency oscillator m . Then, substituting in the integral representation of the Hermite polynomials, we get

$$H_n(x) = \frac{n!}{2\pi i} \int_c dz \frac{e^{2zx - z^2}}{z^{n+1}}, \quad (\text{A8})$$

and doing the integration over x and y in Eq. (A7), we obtain

$$B_m = \frac{D v! u!}{(2\pi i)^2} \pi (1 - e^{-\mu}) \exp[-\frac{1}{2}q^2(1 - e^{-\mu})] \int_c dz \int_c dw \frac{\exp[2e^{-\mu}zw - q(1 - e^{-\mu})(z + w)]}{z^{v+1} w^{u+1}}. \quad (\text{A9})$$

Using the series expansion

$$\exp(2e^{-\mu}zw) = \sum_{n=0}^{\infty} \frac{(2e^{-\mu}zw)^n}{n!} \quad (\text{A10})$$

and the contour integration

$$\int_c dz \frac{f(z)}{z^{v-n+1}} = \frac{2\pi i f^{(v-n)}(0)}{(v-n)!}, \quad (\text{A11})$$

where $f^{(v-n)}(0)$ is the $(v-n)$ th derivative of $f(z)$ evaluated at $z=0$, we find that Eq. (A9) becomes

$$B_m = \exp[-\frac{1}{2}q^2(1 - e^{-\mu}) - \frac{1}{2}\mu] \left[\frac{u! v!}{2^{u+v}}\right]^{1/2} (-1)^{u+v} \sum_{n=0}^{v,u} \frac{(2e^{-\mu})^n [q(1 - e^{-\mu})]^{v+u-2n}}{n! (v-n)! (u-n)!}. \quad (\text{A12})$$

If we next substitute $q = \sqrt{2}S$ and use

$$(1-x)^n = \sum_{p=0}^n \frac{(-1)^p n! x^p}{p! (n-p)!}$$

in Eq. (A12), then we obtain

$$B_m = (-1)^{u+v} \sqrt{v! u!} \sum_{n=0}^{v,u} \sum_{p=0}^{v+u-2n} \frac{(-1)^p (v+u-2n)! (\sqrt{S})^{v+u-2n}}{n! p! (v-n)! (u-n)! (v+u-2n-p)!} \exp[-S(1 - e^{-\mu}) - (n+p + \frac{1}{2})\mu]. \quad (\text{A13})$$

The summation over n in Eq. (A13) is only up to the lowest integer value of u or v . If we let $v = u = 0$ and $m \rightarrow j$ in Eq.

(A13), then we find B_j of Eq. (A3) to be given by

$$B_j = \prod_i \exp[-S_j(1 - e^{-\mu_j})], \quad (\text{A14})$$

where $\mu_j = i\omega_j t$, $S_j = q_j^2/2$, and $q_j = \sqrt{\alpha_j} d_j$. Substituting Eqs. (A13) and (A14) into Eq. (A2), we get

$$\begin{aligned} Z_{a,u;a,v} = & -i(-1)^{u+v} \sqrt{u!v!} \\ & \times \sum_{n=0}^{v,u} \sum_{p=0}^{v+u-2n} \frac{(-1)^p (v+u-2n)! (\sqrt{S'})^{v+u-2n}}{n!p!(v-n)!(u-n)!(v+u-2n-p)!} \\ & \times \int_0^\infty dt \exp\{-i[\omega_{ba} - \omega_1 + (n+p-v_m)\omega_m]t\} \exp\left[-\sum_j S_j(1 - e^{-i\omega_j t}) - S'(1 - e^{i\omega_m t}) - \gamma t\right]. \end{aligned} \quad (\text{A15})$$

If we now use a short-time approximation,¹⁷⁻¹⁹ Eq. (A15) becomes

$$\begin{aligned} Z_{a,u;a,v} = & -i(-1)^{v+u} \sqrt{u!v!} \sum_{n=0}^{v,u} \sum_{p=0}^{v+u-2n} \frac{(-1)^p (v+u-2n)! (\sqrt{S'})^{v+u-2n}}{n!p!(v-n)!(u-n)!(v+u-2n-p)!} \\ & \times \int_0^\infty dt \exp\{-i[\omega_{MA} - \omega_1 + (n+p-v)\omega_m]t\} \\ & \times \exp\left[-S_m(1 - e^{-i\omega_m t}) - \left(\frac{\sum_j S_j \omega_j^2}{2}\right)t^2\right], \end{aligned} \quad (\text{A16})$$

where $\omega_{MA} = \omega_{ba} + \sum_j S_j \omega_j$ is the frequency of the maximum of the electronic absorption, $(8 \ln 2 \sum_j S_j \omega_j^2)^{1/2}$ is the full width at half maximum for the absorption, and we have assumed that

$$\frac{1}{2} \sum_j S_j \omega_j^2 t^2 \gg \gamma t.$$

The temperature effect on the RRS can easily be included by changing $\sum_j S_j \omega_j^2 \rightarrow S\omega^2[2n(\omega) + 1]$,¹⁷⁻¹⁹ where ω is the average phonon frequency coupled to the F -center electron, S is the electron-phonon-coupling constant, and $n(\omega)$ is the population at the average phonon frequency.

¹F. Luty, *Cryst. Lattice Defects Amorph. Mater.* **12**, 343 (1985); F. Rong, Y. Yang, and F. Luty, *Cryst. Lattice Defects Amorph. Mater.* (to be published).

²*Physics of Color Centers*, edited by W. B. Fowler (Academic, New York, 1968).

³Y. Yang and F. Luty, *Phys. Rev. Lett.* **51**, 419 (1983).

⁴K. T. Tsen, G. Halama, and F. Luty, *Phys. Rev. B* **36**, 9247 (1987).

⁵Y. Yang, W. von der Osten, and F. Luty, *Phys. Rev. B* **32**, 2724 (1985).

⁶G. Halama, K. T. Tsen, S. H. Lin, F. Luty, and J. B. Page, *Phys. Rev. B* **39**, 13457 (1989).

⁷Th. Förster, *Ann. Phys. (Leipzig)* **2**, 55 (1948).

⁸D. L. Dexter, *J. Chem. Phys.* **21**, 836 (1953).

⁹W. B. Fowler (private communication). The calculation by Fowler was a comparison of the *absolute* magnitude of the electronic to vibrational energy transfer rate for the 0→4 transition (in the Forster-Dexter (Refs. 7 and 8) or dipole-dipole model) to the radiative emission rate of the F -center electron. In the present paper we compare the *relative* magnitudes of the electronic to vibrational energy transfer (in our supermolecule model) in order to fit the temperature dependence of our Raman spectra.

¹⁰Y. Fujimura and S. H. Lin, *J. Chem. Phys.* **70**, 247 (1979).

¹¹S. H. Lin and H. Eyring, *Proc. Nat. Acad. Sci. U.S.A.* **74**, 3623 (1977); A. Boeglin, B. Fain, and S. H. Lin, *J. Chem.*

Phys. **84**, 4838 (1986).

¹²S. H. Lin, *J. Chem. Phys.* **44**, 3759 (1966).

¹³D. J. Diestler, *J. Chem. Phys.* **60**, 2692 (1974).

¹⁴D. J. Diestler, *Chem. Phys.* **7**, 349 (1975).

¹⁵Qian Zhi-ding, Zhang Xing-Gho, Li Xing-Wen, H. Kono, and S. H. Lin, *Mol. Phys.* **47**, 713 (1982).

¹⁶S. H. Lin, *J. Chem. Phys.* **59**, 4458 (1973).

¹⁷Y. Fujimura, S. H. Lin, and H. Eyring, *Proc. Nat. Acad. Sci. U.S.A.* **77**, 5032 (1980).

¹⁸C. K. Chan and J. B. Page, *Chem. Phys. Lett.* **104**, 609 (1984).

¹⁹C. K. Chan and J. B. Page, *J. Chem. Phys.* **79**, 5234 (1983).

²⁰A. Blumen, S. H. Lin, and J. Manz, *J. Chem. Phys.* **69**, 881 (1978).

²¹The samples used in the experimental measurement have about $2 \times 10^{17} \text{ cm}^{-3}$ F -center concentration and about $1 \times 10^{19} \text{ cm}^{-3}$ CN^- concentration. The anti-Stokes Raman spectra were measured essentially the same way as in Ref. 4, except that the power density of the excitation was kept so low that the effect of the possible repumping of the F center, which is not taken into account in our theoretical calculations, was minimized.

²²C. Kittel, *Introduction to Solid State Physics*, 5th ed. (Wiley, New York, 1976).

²³A. A. Z. Ahmad, H. G. Smith, N. Wakabayashi, and M. K. Wilkinson, *Phys. Rev. B* **6**, 3956 (1972).

²⁴More specifically, the frequency dependence of the vibrational

matrix elements involved in the ν - ν energy-transfer process was neglected in Eq. (29), due to our assumption that $C = \text{const}$. Relaxing this assumption would result in the phonon-frequency density of states being replaced by a local "projected" density of states, in which the density of states is weighted at each phonon frequency by corresponding squared vibrational amplitudes in the vicinity of the defect. The particular amplitudes would depend upon the details and range of the ν - ν coupling. Such local projected densities of states

generally differ significantly from the pure density of states, and they are also sensitive to the phonon perturbations arising from defects. Thus our *fitted* weighted relative phonon density of states should be identified with the appropriate projected density of states for the ν - ν transfer process in this system. Further study of this point would require detailed modeling of the perturbed lattice dynamics and is beyond the scope of the present work.